

Optical detection of the spin state of a single nucleus in silicon

 Kai-Mei C. Fu,* Thaddeus D. Ladd, Charles Santori,[†] and Yoshihisa Yamamoto[‡]
Quantum Entanglement Project, ICORP, JST, Edward L. Ginzton Laboratory, Stanford University, Stanford, California 94305-4085, USA

(Received 12 November 2003; published 9 March 2004)

We propose a method to optically detect the spin state of a ^{31}P nucleus embedded in a ^{28}Si matrix. The nuclear-electron hyperfine splitting of the ^{31}P neutral-donor ground state can be resolved via a direct frequency discrimination measurement of the ^{31}P -bound exciton photoluminescence using single-photon detectors. The measurement time is expected to be shorter than the optically modified lifetime of the nuclear spin at 4 K and 10 T.

DOI: 10.1103/PhysRevB.69.125306

PACS number(s): 76.70.Hb, 03.67.Lx, 71.35.-y, 78.67.-n

I. INTRODUCTION

The spin qubit embedded in a crystalline host is an attractive choice for solid-state quantum computation due to its long coherence time. The inevitable cost of the spin qubit's isolation from the environment is the difficulty of measuring its quantum state. Recently, single-molecule optical spectroscopy has proven to be a successful way to detect individual electronic states at a nitrogen-vacancy defect site in diamond¹ and individual nuclear resonances in molecular crystals.² Spin states in semiconductors, however, have yet to be measured, despite promising semiconductor-based quantum computation proposals.^{3,4} The ability to detect a single-nuclear-spin state in a semiconductor, in particular silicon, would be an important advance in this field where highly developed fabrication techniques already exist and single impurities can be placed with an accuracy up to 1 nm.⁵

Optical readout of the nuclear spin state is an attractive alternative to previously proposed single-nuclear-spin measurements. The proposal of Kane,^{3,6} in which qubits are encoded as the spin state of single embedded ^{31}P nuclei, proposes to solve the single-nuclear-spin measurement problem by adiabatically transferring the nuclear-spin state to the spin of the electron bound to the ^{31}P impurity and measuring the electron's spin-correlated charge state with a single-electron transistor (SET). In practice, however, charge fluctuations produced by the SET couple back to the ^{31}P nucleus via the electron's strong hyperfine interaction, leading to a decoherence source that is not present in bulk silicon. Magnetic resonance force microscopy has approached single-electron-spin sensitivity, but experimental results thus far have shown that this probe induces spin relaxation more quickly than the needed measurement time,⁷ casting doubts on proposals that seek its use for quantum computation.⁸ The use of ensembles of ^{29}Si nuclei in bulk silicon with no metallic gates has been proposed,⁴ but this scheme replaces the measurement problem with the challenge of achieving high nuclear polarization in order to maintain scalability. In this paper, we propose an all-optical method to determine the nuclear spin state of an isolated ^{31}P impurity in bulk silicon. This method's incorporation into silicon-based quantum computation architectures could ease these difficulties.

II. BOUND EXCITON HYPERFINE STATES

In semiconductors, free excitons can be bound to donor and acceptor impurity sites, forming bound excitons. When a

bound exciton (BE) decays radiatively to a neutral impurity state, its linewidth is characteristically narrow due to the localization of the exciton.⁹ If the hyperfine interaction between the impurity nucleus and either the neutral-impurity-bound carrier or the impurity BE is sufficiently strong, the nuclear state of the impurity can be determined via the BE photoluminescence (PL) energy. The particular case of the ^{31}P donor in a ^{28}Si matrix is treated below.

In a magnetic field, the ground state of the ^{31}P BE, denoted (P^0, X) , is split into four hole Zeeman levels. The ground state of the neutral donor P^0 is split into two electron Zeeman levels.¹⁰ These levels are illustrated in Fig. 1.

We assume a large applied magnetic field (≥ 0.01 T) such that the electron-hole Zeeman interaction is much greater than the hyperfine interaction.

The P^0 state is described by effective mass theory (EMT), where the total wave function $\psi_e(\mathbf{r})$ of the donor electron is given by

$$\psi_e(\mathbf{r}) = \frac{1}{\sqrt{6}} \sum_{j=1}^6 F_j(\mathbf{r}) \varphi_j(\mathbf{r}), \quad (1)$$

in which F_j is the hydrogenic envelope function and φ_j is the Bloch function of the j th conduction band minimum in silicon.¹¹ Both the Bloch and envelope functions are s like, so the dominant part of the hyperfine interaction is the Fermi contact term¹²

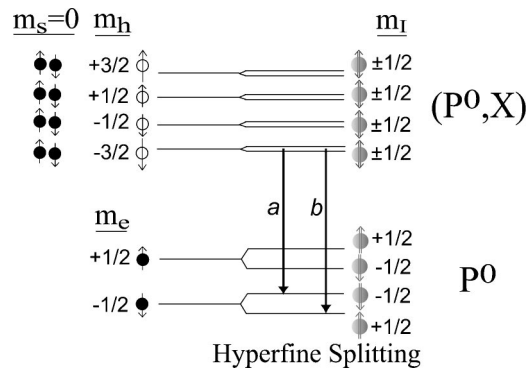


FIG. 1. Energy diagram for the neutral donor (P^0) and its bound exciton (P^0, X) in a magnetic field. The (P^0, X) state is populated via capture of a free exciton. The ^{31}P nuclear state can be determined by the energy difference between a and b .

$$\mathcal{H}_C = -\frac{\mu_0}{4\pi} g_0 \mu_B \hbar \gamma_n \frac{8\pi}{3} \mathbf{I} \cdot \mathbf{S} \delta(\mathbf{r}), \quad (2)$$

where g_0 is the free-electron g factor, γ_n is the ^{31}P gyromagnetic ratio, \mathbf{I} is the nuclear spin operator, and \mathbf{S} is the electron spin operator. When an exciton is bound to the neutral-donor site, the two electrons form an antisymmetric spin-singlet state.^{13,14} Consequently, the hyperfine splitting of the BE is determined only by the spin of the bound hole. Since the hole Bloch function is p -like, the Fermi contact term is negligible, and assuming that the envelope function is s -like, the orbital and dipolar terms will be much smaller than the P^0 contact hyperfine splitting. Thus, the energy difference between the transitions a and b of the (P^0, X) PL, shown in Fig. 1, is determined entirely by the hyperfine splitting of the P^0 state. From Eq. (2), this splitting is

$$\Delta E_{\text{HF}, P^0} = \frac{\mu_0}{3} g_0 \mu_B \gamma_n \hbar |\psi_e(0)|^2. \quad (3)$$

A hyperfine splitting of the 60 MHz site has been determined via electron spin resonance.¹⁵ This splitting has also been calculated with reasonable accuracy using a corrected envelope function to account for the discrepancy in the observed and EMT ionization energies.^{11,16}

The (P^0, X) state in Si decays primarily via a nonradiative Auger process with a lifetime of 300 ns.¹⁷ However, there exists a zero-phonon radiative channel with a lifetime of 2 ms.¹⁷ If the PL linewidth of a single ^{31}P donor impurity is lifetime broadened, it would be approximately 3 MHz, which is much smaller than the hyperfine splitting of 60 MHz. Experimentally, the PL linewidth from an ensemble of ^{31}P impurities was measured to be less than 150 MHz at 2 K, which includes an inhomogeneous broadening effect and was limited by the spectrometer resolution.⁹ Lacking any further knowledge of the actual homogeneous linewidth, we consider below the worst case situation in which the BE PL has a homogeneous phonon broadened linewidth of 150 MHz.

III. OPTICAL MEASUREMENT

After Auger recombination, the electron-hole recombination energy is imparted to the second electron, which is ionized. To ensure a fast recapture process of the donor electron and formation of the BE, one can optically excite free conduction electrons with above-band excitation. Due to Coulombic attraction, free carriers will form free excitons which can bind to the neutral donor. A modest pump power of less than 100 W/cm² will create a bound exciton from an ionized donor in less than 1 ns.^{18–20} The hole spin will equilibrate within the BE lifetime,¹⁰ and in a magnetic field of 10 T at 4 K, the probability for it to occupy the lowest Zeeman level is 80%. Thus, approximately 400 photons/s are emitted at the desired transitions a and b in Fig. 1.

The extraction of an emitted photon out of the high-refractive-index Si substrate as a well-collimated beam for optical detection is important. For this purpose, one can incorporate a planar distributed Bragg reflector (DBR) cavity, as shown in Fig. 2(a), at the center of which a ^{31}P impurity is embedded. The cavity modifies the radiation pattern and

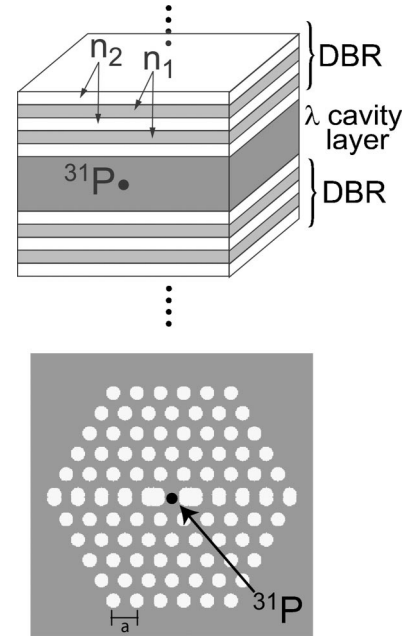


FIG. 2. (a) DBR planar cavity including a ^{31}P impurity at the center of the one-wavelength-thick optical cavity layer. (b) Two-dimensional photonic crystal structure including a ^{31}P impurity at the central defect. The lattice spacing is $a = 0.2847\lambda$. The figure is drawn to scale (Ref. 21).

concentrates the emitted power in the normal direction. With high and low DBR refractive indices $n_1 = 3.0$ and $n_2 = 1.5$, the output coupling efficiency (β factor) into a beam emitted in a normal direction can be as high as 0.8 for a random dipole orientation.²² This efficiency is achieved at the cost of a decreased radiative decay rate by a factor of 3.²² The overall number of PL photons available for optical detection would then be $400 \times 0.8/3 \approx 100$ photons/s.

Alternatively, a two-dimensional (2D) photonic crystal structure [Fig. 2(b)] can simultaneously enhance the output coupling efficiency and the radiative decay rate. A detailed analysis based on the finite-difference time domain (FDTD) method predicts that an optical mode volume of $0.8(\lambda/n)^3$, a Q value of 45 000, a spontaneous emission decay rate enhancement (Purcell) factor of 4000, and a β factor of 1 can be achieved.²¹ Assuming a Purcell factor of 1000, the expected photon flux in this case is 4×10^5 photons/s.

In order to find the measurement time needed to determine the nuclear spin state, we calculate the signal-to-noise ratio for direct frequency detection. In the scheme illustrated by Fig. 3, the BE PL is collected and sent to input a of a

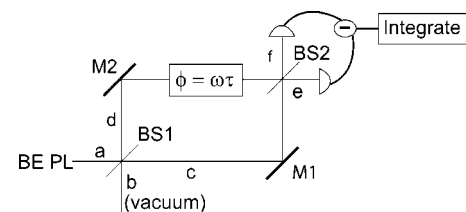


FIG. 3. Mach-Zehnder interferometer for frequency discrimination of BE PL.

Mach-Zender interferometer. The signal is split by the first beam splitter into arms c and d , which have a phase difference of $\omega\tau$. Arms c and d are recombined at the second beam splitter, and the photons in outputs e and f are detected by single-photon detectors. The photocurrents are then subtracted, and the resulting current is time integrated.

We denote the mean frequency of the input state as $\omega_{\pm} = \omega_0 \pm \Delta\omega/2$, where ω_0 is the hyperfine doublet-center frequency and $\hbar\Delta\omega = \Delta E_{\text{HF},P^0}$. Assuming a Lorentzian spectral line shape with full width at half maximum γ , the average integrated single-photon current is proportional to

$$\langle I_{\pm} \rangle = e^{-\gamma\tau/2} \cos(\omega_{\pm}\tau). \quad (4)$$

The variance of the current is proportional to

$$\langle \Delta I_{\pm}^2 \rangle = \langle I_{\pm}^2 \rangle - \langle I_{\pm} \rangle^2 = 1 - e^{-\gamma\tau} \cos^2(\omega_{\pm}\tau). \quad (5)$$

When the interferometer is biased so that $\omega_0\tau = (m + \frac{1}{2})\pi$, the sign of the average difference photocurrent is directly correlated to the state of the nucleus. The difference in the integrated current between the nuclear states is the effective signal amplitude, so the amplitude signal-to-noise ratio for such a frequency detection scheme is given by

$$\frac{S}{N} = \frac{\left| \sin\left(\frac{1}{2}\Delta\omega\tau\right) - \sin\left(-\frac{1}{2}\Delta\omega\tau\right) \right|}{\sqrt{\cos^2\left(\frac{1}{2}\Delta\omega\tau\right) + e^{\gamma\tau} - 1}} \sqrt{\mathcal{N}}, \quad (6)$$

in which \mathcal{N} is the total number of photons collected. The maximum signal-to-noise ratio, corresponding to the delay $\tau = 2$ ns, is 0.29 for one photon assuming a PL linewidth of 150 MHz. If 100 photons per second are collected from a DBR planar cavity, the minimum integration time needed for a signal-to-noise ratio of unity is approximately 0.1 s. If we assume an enhanced spontaneous emission decay rate with a 2D photonic structure mentioned above and a collection efficiency of 0.5, the minimum integration time is reduced to approximately 10^{-5} s.

If the 150 MHz linewidth of the bulk BE PL is due to inhomogeneous broadening, the situation improves significantly. In this case, the lifetime-limited linewidth of 3 MHz is much narrower than the hyperfine splitting. The BE PL center frequency for the isolated impurity can be experimentally determined with this interferometer and the signal-to-noise ratio for a single photon would be 5.

Any practical detection scheme will suffer from detector efficiency and dark count rates. However, negligible dark count rates and a detection efficiency of 0.4 can be obtained at 1.1 μm with a superconducting transition edge sensor²³ (TES). The effect of finite detector efficiency η_d is to decrease the signal-to-noise ratio by $\sqrt{\eta_d}$, extending the measurement time. Alternatively, it may be possible for the signal photons at 1.1 μm to be upconverted to 0.7 μm by a periodically poled LiNbO₃ waveguide and then detected by a Si avalanche photodiode (APD).²⁴ An overall efficiency higher than 0.6 with dark count rates of 100 counts/s is theoretically possible with this detector.

IV. NUCLEAR RELAXATION

Sufficient integration of the luminescence signal measures the nuclear spin state only if that state is stable over a sufficient number of excitation/luminescence cycles. In the case of ³¹P nuclei in silicon, it is known from electron spin resonance (ESR) experiments that the equilibrium nuclear spin relaxation time T_1 of isolated ³¹P nuclei exceeds 10 h at 1.25 K and 0.8 T.²⁵ Such a long T_1 of solid-state nuclei is a combined consequence of the small number of nuclear interactions and a small density of states to which the nuclear Zeeman energy may be transferred. Cross relaxation with the phosphorous-bound electron, induced by the hyperfine interaction with the emission of a phonon, is also a slow process. It was measured to be 5 h at 1.25 K and 0.8 T and should theoretically scale to 30 s at 4 K and 10 T.²⁵ Since the P⁰ ground state only lasts nanoseconds before each optical re-excitation in this scheme, these already long equilibrium relaxation times are negligible. The nucleus may only be appreciably destabilized by the rapid optical excitations we introduce.

We first argue that nuclear spin relaxation due to optically excited, delocalized conduction electrons is not expected to be a significant effect. The number of conduction electrons required for neutralization of the Auger-ionized donors in 1 ns is approximately 10^{13} cm^{-3} , assuming a 4 K electron capture cross section of $4 \times 10^{-11} \text{ cm}^2$.²⁶ At this temperature, electrons are expected to thermalize quickly, in which case the T_1 theory described in Ref. 12 is applicable. This theory predicts a T_1 greater than 10^6 s. Even ²⁹Si in heavily doped ($> 10^{17} \text{ donors/cm}^3$) silicon has a measured T_1 in excess of 200 min at 4 K;^{27,28} the T_1 corresponding to ³¹P nuclei would only be shorter by a factor of about $\gamma_{29\text{Si}}^2/\gamma_{31\text{P}}^2 = 4$, still leaving this time scale unimportant. An argument that T_1 due to free excitons should also be negligibly long follows a similar reasoning, since only the spin of the s -like electron interacts appreciably with the nucleus, and Boltzmann statistics may still be assumed.

Of greater concern is the probability of a nuclear spin flip during the capture of a free electron following the Auger process. Such a nuclear flip arises in second-order perturbation theory, in which a virtual electron capture and a virtual electron-nuclear spin flip-flop in the neutral-donor state occur concurrently with the energy compensated by the real emitted phonon. To estimate the probability of such an event, we note that the energy cost of a hyperfine-induced electron-nuclear spin flip-flop (approximately the 1.2 meV Zeeman energy of the neutral-donor spin) is substantially smaller than the donor binding energy (45 meV). We may therefore assume that the density-of-states factors in Fermi's golden rule are unchanged between the first- and second-order processes and that they are independent of the initial spin state. We also assume that the optical excitation of free carriers is not spin selective, and since T_1 for these carriers exceeds the capture time, this implies that the initial spin polarizations are approximately equal. It follows from these assumptions that the probability ratio between the first- and second-order processes is well approximated by the ratio between their matrix elements. The second-order matrix element for an electron-

nuclear flip-flop process, assuming without loss of generality that the nucleus begins in the $|\downarrow\rangle$ state, may be written as

$$|V_{P^+\uparrow\downarrow\rightarrow P^0\downarrow\uparrow}^{(2)}|^2 = \left| \frac{\langle P^+\uparrow\downarrow | \mathcal{H}_N | P^0\uparrow\downarrow \rangle \langle P^0\uparrow\downarrow | \mathcal{H}_C | P^0\downarrow\uparrow \rangle}{E_{P^0\downarrow\uparrow} - E_{P^0\uparrow\downarrow}} \right|^2, \quad (7)$$

in which $|P^+\uparrow\downarrow\rangle$ describes the ionized donor and $|P^0\uparrow\downarrow\rangle$ describes the neutral donor with electron spin up and nucleus spin down. These states are the only important ones for nuclear destabilization, since the $|P^0\downarrow\downarrow\rangle$ state is unperturbed by \mathcal{H}_C . The unperturbed eigenenergy difference between the intermediate and final state, $E_{P^0\downarrow\uparrow} - E_{P^0\uparrow\downarrow}$, is a sum of the electron Zeeman term, the nuclear Zeeman term, and $\Delta E_{\text{HF},P^0}$; the electron Zeeman term dominates this sum. The Hamiltonian term \mathcal{H}_N refers to the interaction leading to the capture of the free electron; thus, a first-order matrix element for a neutralization process without a flip-flop is written as

$$|V_{P^+\uparrow\downarrow\rightarrow P^0\uparrow\downarrow}^{(1)}|^2 = |\langle P^+\uparrow\downarrow | \mathcal{H}_N | P^0\uparrow\downarrow \rangle|^2. \quad (8)$$

We assume that this Coulombic process has no spin selectivity. It follows that the probability per transition of a flip-flop may be written as

$$\frac{|V_{P^+\uparrow\downarrow\rightarrow P^0\downarrow\uparrow}^{(2)}|^2}{|V_{P^+\uparrow\downarrow\rightarrow P^0\uparrow\downarrow}^{(1)}|^2 + |V_{P^+\downarrow\downarrow\rightarrow P^0\downarrow\downarrow}^{(1)}|^2 + |V_{P^+\uparrow\downarrow\rightarrow P^0\downarrow\uparrow}^{(2)}|^2} \approx \frac{1}{2} \left| \frac{\langle P^0\uparrow\downarrow | \mathcal{H}_C | P^0\downarrow\uparrow \rangle}{E_{P^0\downarrow\uparrow} - E_{P^0\uparrow\downarrow}} \right|^2 = \frac{1}{2} \left(\frac{\Delta E_{\text{HF},P^0}}{g\mu_B B_0} \right)^2. \quad (9)$$

This probability can be seen from an alternative viewpoint: if we use second-order time-independent perturbation theory to calculate the mixing of the $|P^0\uparrow\downarrow\rangle$ and $|P^0\downarrow\uparrow\rangle$ states due to the flip-flop terms of \mathcal{H}_C and presume that capture rates to these perturbed states are the same as to the unperturbed states, the same probability is obtained.

The free-exciton-capture process leads to a similar second-order probability for nuclear randomization. In this case, however, the binding energy of the free exciton to the neutral donor is only somewhat larger than the electron Zeeman energy, so the density-of-states factors in the transition rates can become important. However, we do not expect this correction to alter the per-transition probability by more than a factor of order unity. We thus estimate that at 10 T, the probability of a nuclear flip for each free-exciton-capture and free-electron-capture process is approximately twice the result of Eq. (9): $(60 \text{ MHz}/280 \text{ GHz})^2 = 5 \times 10^{-8}$. The consequences of this probability will be discussed shortly.

A nuclear spin flip can also occur in a similar manner during a free-exciton capture or BE Auger decay due to the BE (hole-nuclear) hyperfine interaction. This process is less important because the BE hyperfine interaction is much weaker. The magnitude of this interaction, which includes both dipolar coupling and any contribution due to a small s -like component of the hole's Bloch wave function, may be estimated as 2 MHz from the results of muon spin resonance experiments.²⁹ Since the BE Zeeman energy is comparable to that of the bound electron, the probability of a spin flip due

to the BE hyperfine coupling is smaller by the approximate factor $(2 \text{ MHz}/60 \text{ MHz})^2 \sim 10^{-3}$. Nuclear spin flip due to the P^0 hyperfine coupling during radiative decay has a similar order to that during free-electron capture, but since radiative decay is 10^4 times less frequent than Auger recombination for the DBR planar cavity and 10 times less frequent for the photonic crystal, respectively, this probability may also be neglected.

It is unfortunate that the predominant decay mechanism is nonradiative, since each Auger process increases the probability of nuclear randomization without providing a signal photon. After 2×10^6 excitations, at which point the probability of nuclear randomization exceeds 1/10, we can only expect to have collected and detected 25 photons or 5×10^4 photons with a DBR planar cavity or a 2D photonic crystal, respectively. This still yields a usable signal-to-noise ratio of 1.5 or 65 for the respective geometries. Thus, we expect the measurement-induced lifetime of the single nuclear spin to be long enough to allow for the measurement of the nuclear spin state.

V. DISCUSSION

The optical method proposed here could be scaled to measure individual ^{31}P nuclei in a long array. For example, if a magnetic field gradient is parallel to the nuclear chain, different nuclei can be distinguished optically by the BE PL frequency shift due to the P^0 and (P^0, X) electron-hole Zeeman splitting. Magnetic field gradients on the order of $1 \text{ T}/\mu\text{m}$ can be obtained using a ferromagnetic micromagnet.³⁰ For ^{31}P nuclei spaced 200 \AA apart,³ the BE PL from neighboring nuclei will be separated by 200 MHz. Since every ^{31}P will emit at a different frequency, it will not be possible to use the Mach-Zender interferometer. Instead, the photoluminescence from a single nucleus can be filtered from neighboring nuclei using an interference filter such as a Fabry-Perot étalon. In addition, the transmitted intensity through the filter will vary with the spin state of the nucleus, providing a method to determine the nuclear spin state. In addition, the signal-to-noise ratio will depend slightly on the nuclear spin states of neighboring nuclei whose PL will be partly transmitted through the filter. In Fig. 4(a), the PL frequency spectrum for an arbitrary set of nuclear spin states is shown by the dark black line. The gray line indicates the frequency spectrum when the i th nuclear spin is flipped and it is evident that light transmitted through the étalon will be different for these two states. For randomly distributed neighboring nuclear states, the signal-to-noise ratio for a single photon will vary between 0.14 and 0.16 for the filter shown in Fig. 4 in the ideal detection limit. A reasonable signal-to-noise ratio during the spin lifetime is possible if spontaneous emission is sufficiently enhanced in a photonic band-gap cavity for a line defect. In order to illustrate that the signal is relatively unaffected by neighboring nuclear spin states, in Fig. 4(b) we have plotted the two spectra corresponding to the two i th nuclear spin states with neighboring nuclear spins averaged over all possible states.

Alternatively, in the photonic band-gap cavity case, spatially resolved excitation and collection may also be feasible

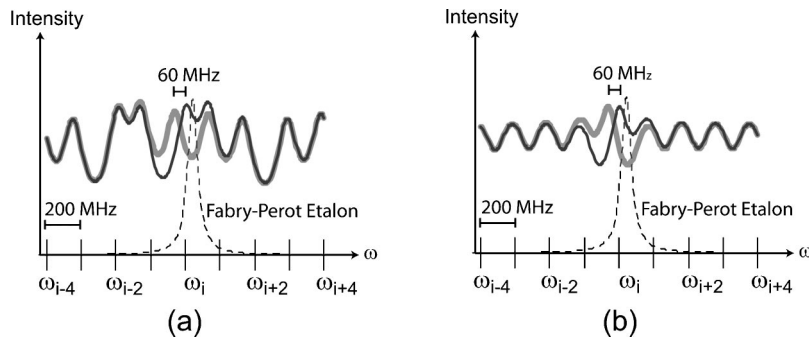


FIG. 4. PL intensity for a ^{31}P array in a magnetic field gradient. (a) Dark solid line: PL spectrum for randomly oriented ^{31}P nuclei. Gray line: PL with i th nuclear spin flipped, but neighboring spin states unchanged. Dashed line: transmission function of Fabry-Perot étalon used to read the spin state of i nuclear spin. (b) Neighboring nuclear spins are averaged over all possible spin states.

using a scanning near-field optical microscope (SNOM) which can achieve resolution down to a few tens of nanometers.³¹ Both experimental schemes—SNOM and the use of a magnetic field gradient—would require the design of a photonic band-gap crystal which would enhance the emission of a line defect instead of a point defect. Another challenge facing large-scale optical detection, especially in the field gradient scheme, is the minimization of the optical disturbance on neighboring spins during readout.

VI. CONCLUSION

In summary, we have proposed utilizing the sharp BE PL lines for single-nuclear-spin measurement. We have demonstrated that it is theoretically possible to measure a single donor impurity spin in silicon using currently available technology: a semiconductor microcavity and single-photon de-

tectors. We have analyzed only one type of BE in Si, chosen for its experimentally observed strong hyperfine coupling and narrow PL linewidths. However, bound excitons exist in abundance in most semiconductors. Thus, this technique could be applied to many more systems if the crystal quality is sufficiently high and the hyperfine coupling and photon flux are sufficiently large. We believe this technique holds promise for state readout in quantum computers utilizing nuclear qubits in semiconductors.

ACKNOWLEDGMENTS

This work was partially supported by NTT Basic Research Laboratories. T.D.L. was supported by the Fannie and John Hertz Foundation. K.C.F. was supported by the National Science Foundation. We would like to thank J. Vuckovic for fruitful discussions.

*Electronic address: kaimeifu@stanford.edu

[†]Also at Research Center for Advanced Science and Technology, University of Tokyo, 4-6-1 Komaba, Meguro-ku, Tokyo 153-8904, Japan.

[‡]Also at NTT Basic Research Laboratories, 3-1 Morinosato-Wakamiya Atsugi, Kanagawa, 243-0198, Japan.

¹F. Jelezko *et al.*, *Appl. Phys. Lett.* **81**, 2160 (2002).

²J. Wrachtrup, A. Gruber, L. Fleury, and C. Borczyskowski, *Chem. Phys. Lett.* **267**, 179 (1997).

³B. Kane, *Nature (London)* **393**, 133 (1998).

⁴T.D. Ladd *et al.*, *Phys. Rev. Lett.* **89**, 017901 (2002).

⁵S.R. Schofield *et al.*, *Phys. Rev. Lett.* **91**, 136104 (2003).

⁶B.E. Kane *et al.*, *Phys. Rev. B* **61**, 2961 (2000).

⁷B.C. Stipe *et al.*, *Phys. Rev. Lett.* **87**, 277602 (2001).

⁸G.P. Berman, G.W. Brown, M.E. Hawley, and V.I. Tsifrinovich, *Phys. Rev. Lett.* **87**, 097902 (2001).

⁹D. Karaiskaj *et al.*, *Phys. Rev. Lett.* **86**, 6010 (2001).

¹⁰U. Ziemelis, R. Parsons, and M. Thewalt, *Can. J. Phys.* **60**, 222 (1982).

¹¹W. Kohn, in *Solid State Physics*, edited by R. Seitz and D. Turnbull (Academic, New York, 1957), Vol. 5, pp. 257–320.

¹²A. Abragam, *The Principles of Nuclear Magnetism* (Oxford University Press, Oxford, 1961), Chap. IX, pp. 389–401.

¹³G. Kirczenow, *Can. J. Phys.* **55**, 1787 (1977).

¹⁴P. Dean, W. Flood, and G. Kaminsky, *Phys. Rev.* **163**, 721 (1967).

¹⁵G. Feher, *Phys. Rev.* **103**, 834 (1956).

¹⁶G. Feher, *Phys. Rev.* **114**, 1219 (1959).

¹⁷W. Schmid, *Phys. Status Solidi B* **84**, 529 (1977).

¹⁸G. Schramm, *Phys. Status Solidi A* **125**, K113 (1991).

¹⁹V.N. Abakumov, V.I. Perel', and I.N. Yassievich, *Sov. Phys. Semicond.* **12**, 1 (1977).

²⁰J.D. Cuthbert, *Phys. Rev. B* **1**, 1552 (1970).

²¹J. Vučković and Y. Yamamoto, *Appl. Phys. Lett.* **82**, 2374 (2003).

²²Y. Yamamoto, S. Machida, and K. Igeta, in *Coherence, Amplification, and Quantum Effects in Semiconductor Lasers*, edited by Y. Yamamoto (Wiley, New York, 1991), pp. 561–615.

²³B. Cabrera *et al.*, *Physica B* **280**, 509 (2000).

²⁴C. Langrock, R.V. Roussev, J.R. Kurz, and M.M. Fejer (unpublished).

²⁵G. Feher and E. Gere, *Phys. Rev.* **114**, 1245 (1959).

²⁶P. Norton, T. Braggins, and H. Levinstein, *Phys. Rev. Lett.* **30**, 488 (1973).

²⁷R. Sundfors and D. Holcomb, *Phys. Rev.* **136**, A810 (1964).

²⁸D. Jérôme, *Rev. Mod. Phys.* **40**, 830 (1968).

²⁹T. Mamedov, V. Gorelkin, and A. Stoikov, *Phys. Part. Nucl.* **33**, 519 (2002).

³⁰J.R. Goldman, T.D. Ladd, F. Yamaguchi, and Y. Yamamoto, *Appl. Phys. A: Mater. Sci. Process.* **71**, 11 (2000).

³¹E. Betzig, P.L. Finn, and S.J. Weiner, *Appl. Phys. Lett.* **60**, 2484 (1992).